

Thermal Fractionation and Properties of Different Polyethylene/Wax Blends

M. J. Hato, A. S. Luyt

Department of Chemistry, University of the Free State (Qwaqwa Campus), Phuthaditjhaba 9866, South Africa

Received 23 March 2006; accepted 19 September 2006

DOI 10.1002/app.25494

Published online in Wiley InterScience (www.interscience.wiley.com).

ABSTRACT: The influence of paraffin-wax type and content on the properties of its blends with HDPE, LDPE, and LLDPE was investigated. Melt-mixing of HDPE with wax gave rise to completely miscible blends for both 10 and 20% wax contents. A wax content of 30% gave rise to a partially miscible blend. These observations were supported by the thermal fractionation (stepwise cooling) results. Melt-mixing of LDPE with hard paraffin wax gave rise to a partially miscible blend for all wax contents investigated, while complete miscibility was observed for the 10% oxidized hard paraffin wax containing blend. Complete miscibility was observed for all the LLDPE/A1 wax blends, with A1 wax as an oxidized hard paraffin wax. This indicates possible cocrystalli-

zation of this wax with LLDPE, which was also evident from the thermal fractionation curves. LLDPE blends with hard paraffin wax were, however, partially miscible for all wax contents. All the observations were supported by the surface free energy results. It is further clear from the thermal fractionation results that the presence of wax changed the crystallization behavior of LDPE and LLDPE. Changes in the tensile properties are explained in terms of the miscibility and proposed morphologies of the blends. © 2007 Wiley Periodicals, Inc. *J Appl Polym Sci* 104: 2225–2236, 2007

Key words: polyethylene; paraffin wax; blends; thermal fractionation; DSC; tensile properties

INTRODUCTION

Although much work had been done on the thermal and mechanical properties of polyethylene/wax blends,^{1–11} it is still not clear how the presence of wax influences the crystallization behavior of polyethylene in polyethylene/wax blends. Luyt and Brúll¹⁰ investigated the crystallization behavior of HDPE, LDPE, and LLDPE blended with an oxidized paraffin wax, and conclusively established cocrystallization of the wax and LLDPE from solution. Their results did, however, not clearly show the cocrystallization of the wax with HDPE. Krump et al.¹² described a relationship between HDPE-wax miscibility and the surface free energy of the blends.

Galante et al.¹³ investigated the role of crystallization conditions on the crystallization of blends of different types of polyethylene. When mixing a linear polyethylene with a polyethylene copolymer, they found peaks associated with the melting of linear polyethylene crystals and that of the melting of cocrystals. In some cases, they found endothermic melting peak broadening, which may indicate that a weak

endothermic peak (representing cocrystals) may be buried within the observed broad endothermic peak. Increasing the copolymer concentration will give rise to a greater extent of cocrystallization. The amount of cocrystallization increases with decreasing crystallization temperature. Partial cocrystallization was also found during slow cooling or isothermal crystallization, and this was influenced by the branching composition, molecular structure, and branching distribution of the copolymer. Cocrystallization is slightly favored in the mixtures of unfractionated polydisperse ethylene copolymers. The polydispersity of the linear component, or that of the long-chain branched polyethylene, did not seem to affect the cocrystallization. A major factor governing cocrystallization of mixtures of linear and branched components is the similarity of crystallization rates of the pure components. The proximity of the crystallization rates of the linear and branched polyethylenes will be proportional to the dilution effect of the branched component on the melting temperature of the linear one when crystallized from a homogeneous melt that depends on the melt-mixing thermodynamics as well as possible morphological effects. The effect of this dilution on the initial crystallization temperature of the linear polyethylene, and the type of LLDPE, controls the cocrystallization behavior of slowly crystallized blends.

A number of authors investigated the crystallization behavior of polyethylene blends by a process of step crystallization (SC) from the melt using DSC.^{14–22}

Correspondence to: A. S. Luyt (luytas@qwa.uovs.ac.za).

Contract grant sponsor: The National Research Foundation in South Africa; contract grant number: GUN 2050677.

Contract grant sponsor: The University of the Free State.

Journal of Applied Polymer Science, Vol. 104, 2225–2236 (2007)
© 2007 Wiley Periodicals, Inc.

Müller and Arnal²³ summarized these results and they observed that, in thermal fractionation, the polymer chains are never physically separated, and therefore the technique is sensitive to linear and uninterrupted chain sequences. This implies that thermal fractionation is equally sensitive to both intra- and intermolecular defects. SC induces molecular segregation as a function of the ability that chains or chain segments have to crystallize at specific temperatures, depending on the distribution of sequences. In the case of ethylene/ α -olefin copolymers, the linear and uninterrupted chain sequences will be limited by the comonomer content and its distribution along the chain. In thermal fractionation, the final distribution of melting points depends on how close to equilibrium are the crystals generated, since chain folding occurs beyond a critical number of linear and uninterrupted chain sequences and will most probably be present in a great number of high-melting point thermal fractions. The final heating scan after SC fractionation reveals a series of multiple melting peaks that are a reflection of the multiple mean lamellar thicknesses obtained. They indicate that chain intra- and intermolecular heterogeneities are present in the sample. The highest melting point fraction corresponds to the fusion of the thickest lamellae that are formed by the longest uninterrupted chain sequence. Progressively, shorter sequences will crystallize in progressively thinner lamellae that melt at lower temperatures. Extended chain crystals are not likely formed within high temperature melting fractions of high molecular weight materials because of the prevalence of chain folding. Different authors used different cooling rates during stepwise cooling, but it is generally assumed that cooling rates of $60^{\circ}\text{C min}^{-1}$ or higher are high enough to prevent crystallization during cooling. It was further found that the thermal fractionation process is fundamentally controlled by the comonomer content and its distribution, and is not affected too much by the molecular weight or its distribution, as long as chain diffusion problems are not encountered.

EXPERIMENTAL

Materials

Hard (H1) and oxidized (A1) Fischer-Tropsch paraffin waxes were used in this study. H1 wax has a weight-average molecular weight of 813 g mol^{-1} , polydispersity of 1.25, a melting temperature of 90°C , and a density of 0.94 g cm^{-3} at 25°C . It decomposes at 250°C and is chemically inert. A1 wax is an oxidized straight-hydrocarbon chain paraffin wax with a weight-average molecular weight of 669 g mol^{-1} , a density of 0.95 g cm^{-3} , a melting temperature of 96°C ,

and a C/O ratio 18.8/1. Both waxes were supplied by Sasol Wax.

HDPE, LDPE, and LLDPE were supplied in pellet form by Sasol Polymers. HDPE has an MFI of 8 g/10 min (ASTM D1238), a weight-average molecular weight of $298,615\text{ g mol}^{-1}$, a polydispersity of 9.5, a melting temperature of 130°C , and a density of 0.95 g cm^{-3} . LDPE has an MFI of 7.0 g/10 min (ASTM D1238), a weight-average molecular weight of $309,065\text{ g mol}^{-1}$, a polydispersity of 7.9, a melting temperature of 106°C , and a density of 0.918 g cm^{-3} . LLDPE has an MFI of 1.0 g/min (ASTM D1238), a weight-average molecular weight of $257,367\text{ g mol}^{-1}$, a polydispersity of 4.0, a hexene content of 2.13 mol %, a melting temperature of 124°C , and a density of 0.924 g cm^{-3} .

Methods

HDPE, LDPE, and LLDPE were initially melt-mixed with H1 wax and A1 wax, respectively, in a Brabender Plastograph (screw speed of 30 rpm for 15 min.) at temperatures of 160 (HDPE), 140 (LDPE), and 150 (LLDPE). The blends were prepared in PE/wax w/w ratios of 100/0, 90/10, 80/20, 70/30, and 0/100. The blending was followed by melt-pressing at the same temperatures for 5 min at 90 bar in a hot-melt press.

DSC analyses were performed in a PerkinElmer DSC7 under flowing nitrogen (20 mL min^{-1}). The instrument was calibrated at a heating rate of $10^{\circ}\text{C min}^{-1}$ using the onset temperatures of melting of indium (10.4 mg) and zinc (9.9 mg) standards, as well as the melting enthalpy of indium. Blend samples (mass $\sim 5\text{ mg}$) were sealed in aluminum pans and heated from 25 to 160°C at a heating rate of $10^{\circ}\text{C min}^{-1}$, and cooled at the same rate to 25°C . For the second scan, the samples were heated and cooled under the same conditions. Onset and peak temperatures of melting and crystallization as well as melting and crystallization enthalpies were determined from the second scan. The DSC curves were integrated using a sigmoidal baseline with low- and high-temperature limits of about 90 and 150°C , 50 and 130°C , and 70 and 150°C for HDPE, LDPE, and LLDPE, respectively.

Polymer samples (mass $\sim 5\text{ mg}$) were thermally fractionated using a PerkinElmer DSC7. The thermal history of the samples was removed by heating the polymer samples to 160°C , keeping it there for 5 min. The temperature was then decreased in 4°C steps to 50°C , leaving the sample isothermal for 50 min after each step. A step cooling rate of $100^{\circ}\text{C min}^{-1}$ was used. The fractionated sample was then heated from 25 to 160°C at a heating rate of $10^{\circ}\text{C min}^{-1}$.

A surface energy evaluation system (SEES, Czech Republic), which enables the calculations of surface free energy from contact angle measurements, was used. Benzyl alcohol, aniline, formamide, ethylene glycol, and water were all used as test liquids. The

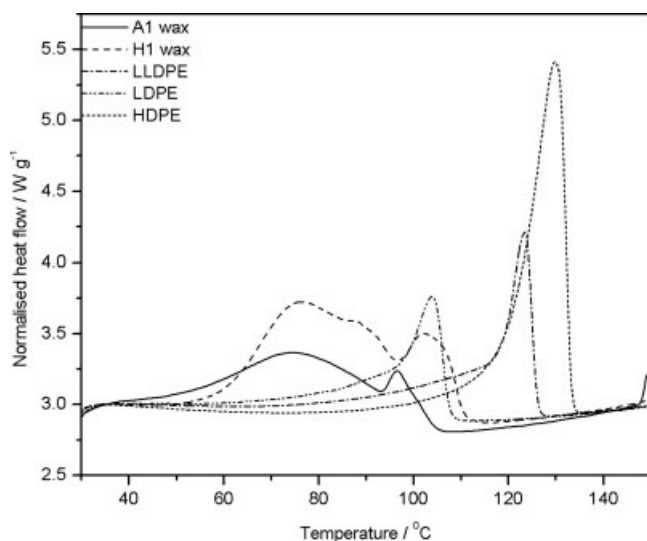


Figure 1 DSC heating curves of pure polyethylenes and waxes.

Owens-Wendt regression method was used for the surface free energy calculations. The ultimate surface free energy results were calculated from at least 15 drops for each test liquid to ensure reproducibility at laboratory temperature.

A Hounsfield H5KS tensile tester was used for the tensile analysis of the samples. The dumbbell samples

were stretched at a speed of 50 mm min^{-1} . The sample length was 75 mm, the thickness (1.0 ± 0.1) mm, and the width 5 mm. The final mechanical properties were evaluated from at least seven different measurements.

RESULTS AND DISCUSSION

Figure 1 shows the DSC curves of pure HDPE, LDPE, LLDPE, H1 wax, and A1 wax. Both A1 wax, which contains carbonyl groups on the backbone chains, and H1 wax, which is a straight-chain hydrocarbon, melt over a broad temperature range.

The DSC curves (not reproduced here) of the 90/10 and 80/20 w/w HDPE/wax blends show only the HDPE melting peak with no indication of the wax melting peak. This is probably due to the incorporation of wax into the crystal lamellae of HDPE. A wax content of 30% gives rise to a partially miscible blend, which results in the development of a lower temperature melting peak in the DSC curve. This suggests that, at high wax content, it is thermodynamically more favorable for the wax to crystallize separately. In the case of HDPE/H1 wax blends, the enthalpy increased with increasing wax content (Table I), indicating an increase in crystallinity with an increase in H1 wax content. Since H1 wax has a chemical struc-

TABLE I
DSC Results of Polyethylenes, Waxes, and Their Blends

Sample	$T_{o,m}/^{\circ}\text{C}$	$T_{p,m} = T_m/^{\circ}\text{C}$	$\Delta H_m/\text{J g}^{-1}$	$T_{o,c}/^{\circ}\text{C}$	$T_{p,c} = T_c/^{\circ}\text{C}$	$\Delta H_c/\text{J g}^{-1}$
A1 wax	55.4	73.9	75.8	91.1	88.0	-58.9
	94.1	96.9		83.9	70.6	
H1 wax	59.4	76.5	178.8	92.9	90.1	-154.6
	88.6	87.5		85.0	79.0	
	97.7	106.4		77.2	68.1	
HDPE	119.6	129.9	154.5	115.5	112.1	-127.9
LLDPE	118.0	123.7	79.7	110.8	108.1	-68.2
LDPE	95.6	104.2	62.7	91.7	88.5	-52.6
HDPE/H1 wax (90/10 w/w)	118.9	131.4	150.6	117.0	113.5	-120.5
HDPE/H1 wax (80/20 w/w)	119.2	129.5	166.7	114.8	112.3	-110.2
HDPE/H1 wax (70/30 w/w)	119.5	128.7	170.5	115.2	112.6	-90.1
HDPE/A1 wax (90/10 w/w)	121.5	131.2	119.1	115.8	112.1	-111.0
HDPE/A1 wax (80/20 w/w)	120.3	129.9	119.8	115.1	112.5	-106.5
HDPE/A1 wax (70/30 w/w)	120.6	129.0	122.8	111.3	108.5	-90.7
LLDPE/H1 wax (90/10 w/w)	121.0	125.7	103.7	109.7	107.5	-54.4
LLDPE/H1 wax (80/20 w/w)	118.1	124.5	95.3	108.5	106.3	-63.4
LLDPE/H1 wax (70/30 w/w)	117.6	123.7	98.3	107.9	105.8	-45.2
LLDPE/A1 wax (90/10 w/w)	119.1	123.9	71.4	107.5	109.5	-45.0
LLDPE/A1 wax (80/20 w/w)	119.4	124.2	67.9	107.5	109.6	-41.1
LLDPE/A1 wax (70/30 w/w)	118.9	124.2	54.8	111.8	109.3	-36.9
LDPE/H1 wax (90/10 w/w)	95.4	104.0	72.1	92.1	88.1	-40.4
LDPE/H1 wax (80/20 w/w)	95.8	103.7	76.9	93.1	90.1	-31.5
LDPE/H1 wax (70/30 w/w)	88.8	103.4	98.1	95.6	92.1	-37.7
LDPE/A1 wax (90/10 w/w)	97.5	104.7	72.5	90.4	87.0	-57.0
LDPE/A1 wax (80/20 w/w)	94.0	102.0	63.5	90.1	86.8	-38.4
LDPE/A1 wax (70/30 w/w)	94.4	101.0	58.6	89.6	86.6	-35.1

$T_{o,m}$, $T_{p,m}$, $T_{o,c}$, $T_{p,c}$, ΔH_m , and ΔH_c are respectively the onset temperature of melting, peak temperature of melting, onset temperature of crystallization, peak temperature of crystallization, melting enthalpy, and crystallization enthalpy.

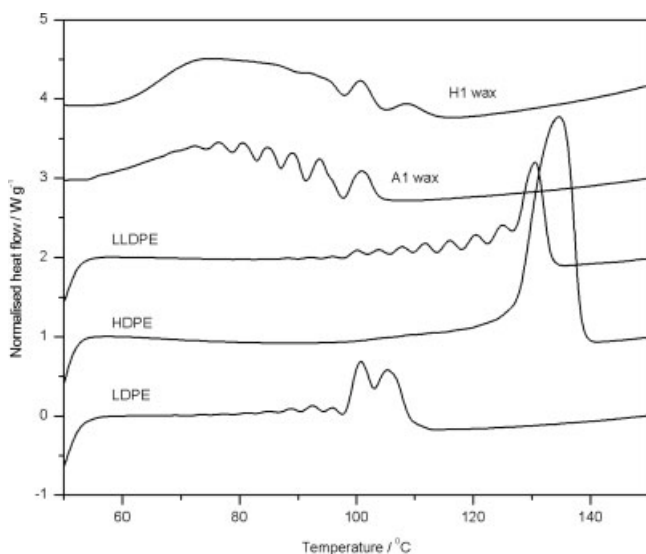


Figure 2 DSC heating curves, after thermal fractionation, of pure polyethylenes and waxes.

ture similar to HDPE, one may assume that 100% crystalline wax has the same enthalpy as 100% crystalline polyethylene. In our case, the pure H1 wax has a higher melting enthalpy, which explains the increased enthalpy (crystallinity) of these blends. In the case of A1 wax blends, the melting enthalpies of the blends are lower than that of HDPE, but slightly increase with an increase in wax content. This is the result of the smaller enthalpy value of A1 wax when compared with that of pure HDPE (Table I). The increased enthalpy (or crystallinity) with increasing wax content is probably the result of cocrystallization of the wax with HDPE. Although one may assume that the wax chains do not undergo chain folding during crystallization, we are of the opinion that the wax chains are short enough (~ 9 nm, compared to an approximate PE lamellar thickness of 10 nm) to be incorporated as straight chains into the HDPE lamellae. In previous research by our group,¹⁰ such cocrystallization from solution was conclusively established.

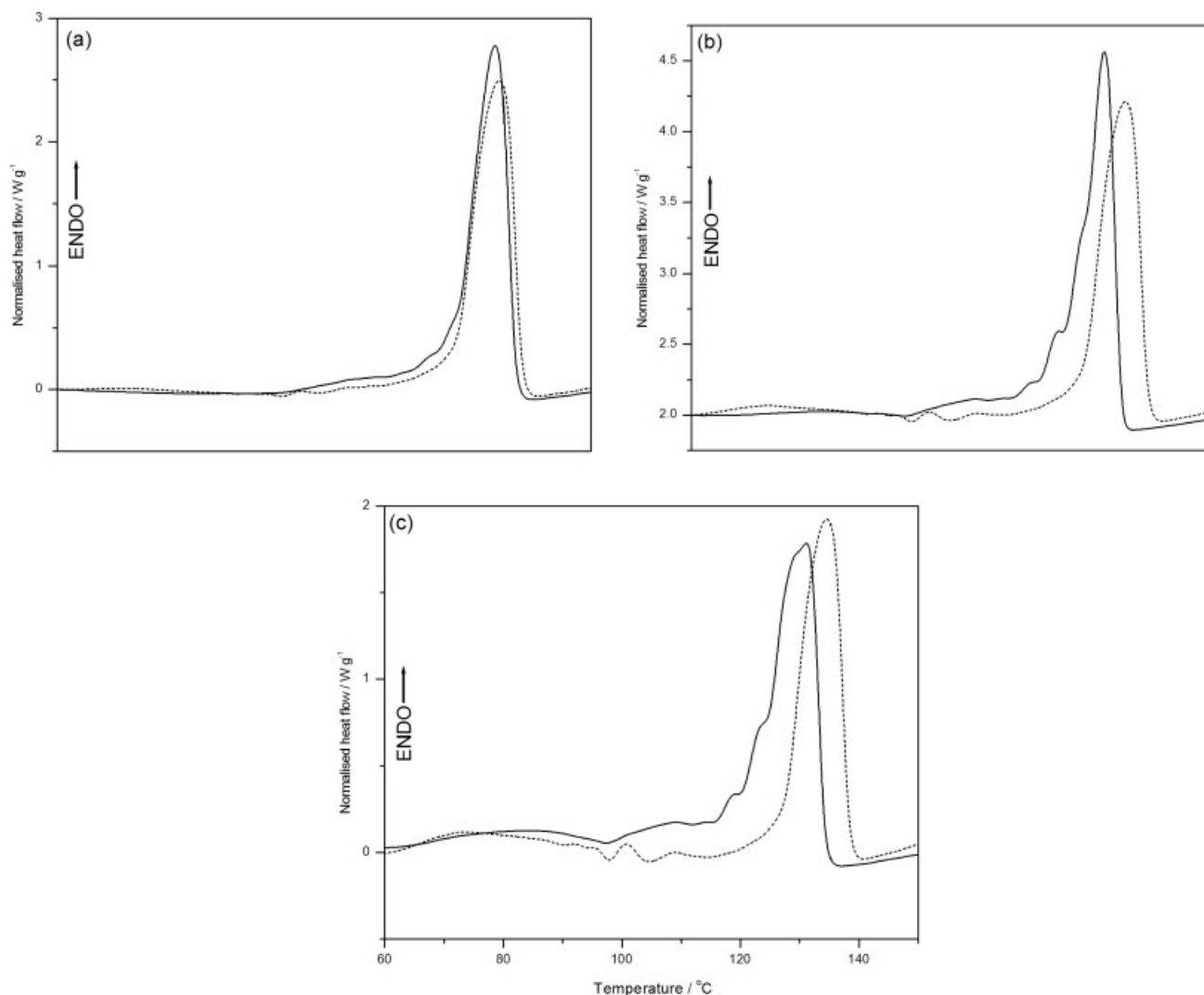


Figure 3 DSC heating curves, after thermal fractionation, of HDPE/H1 wax blends (solid line—experimental curves, broken line—calculated curves): (a) 90/10, (b) 80/20, and (c) 70/30 w/w.

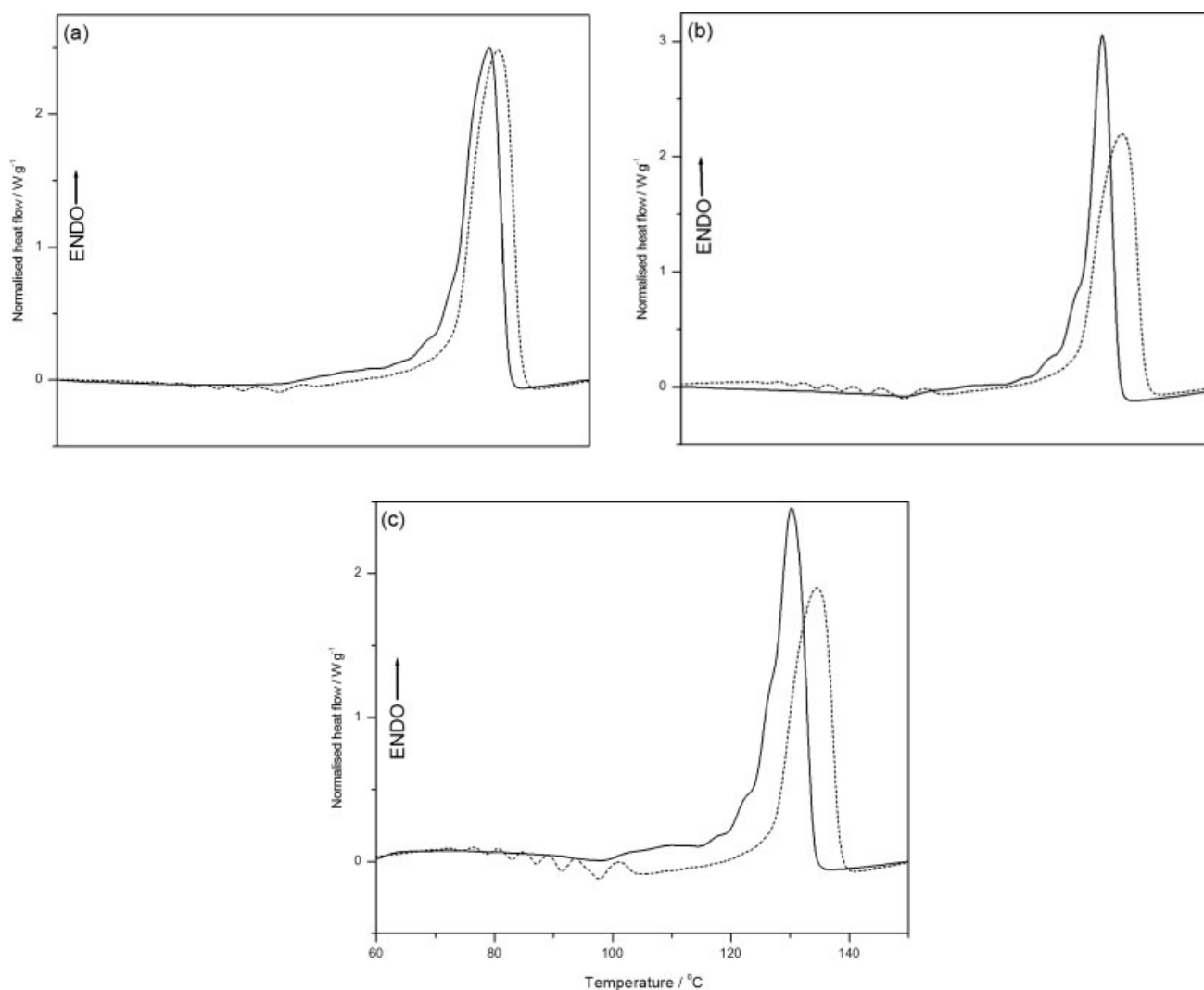


Figure 4 DSC heating curves, after thermal fractionation, of HDPE/A1 wax blends (solid line—experimental curves, broken line—calculated curves): (a) 90/10, (b) 80/20, and (c) 70/30 w/w.

In the DSC curves (not reproduced here) of the 90/10 w/w LDPE/wax blends, only one endothermic peak is observed, which shows that LDPE and wax are miscible in the crystalline phase in this concentration region. For 20 and 30% of both waxes, another small broad endothermic peak is observed in the temperature range of 70–85°C, which corresponds to the main melting peak of pure wax. This is probably the melting peak of the fraction of the wax, which is not miscible with LDPE, indicating that LDPE is only partially miscible with both waxes at higher wax contents. An increase in enthalpy with increasing H1 wax content is observed. Since H1 wax has linear hydrocarbon chains of low molecular weight, some of these chains probably cocrystallize with linear sequences of the LDPE chains, favoring the crystallization process.²⁴ This can also be explained by H1 wax having a melting enthalpy higher than that of pure LDPE (Table I). However, a decrease in enthalpy values is

observed with increasing A1 wax content, despite the fact that A1 wax has a somewhat higher crystallinity than LDPE. A possible reason for this decrease in enthalpy with increasing wax content is the fact that A1 wax starts crystallizing at the same temperature as LDPE. The presence of wax crystals may inhibit LDPE chain mobility, giving rise to lower crystallinity.

LLDPE blended with A1 wax shows only one DSC melting peak (not reproduced here). This behavior indicates that LLDPE and A1 wax are miscible in the crystalline phase at all compositions in the range of compositions investigated. This observation is in line with those by Luyt and Brüll,¹⁰ who investigated the crystallization of LLDPE/A1 wax blends from solution. Different behavior was observed when H1 wax was used. For all wax concentrations, three peaks were observed. One of them corresponds to that of LLDPE and the other two to those of H1 wax, indicating only partial miscibility of H1 wax and LLDPE

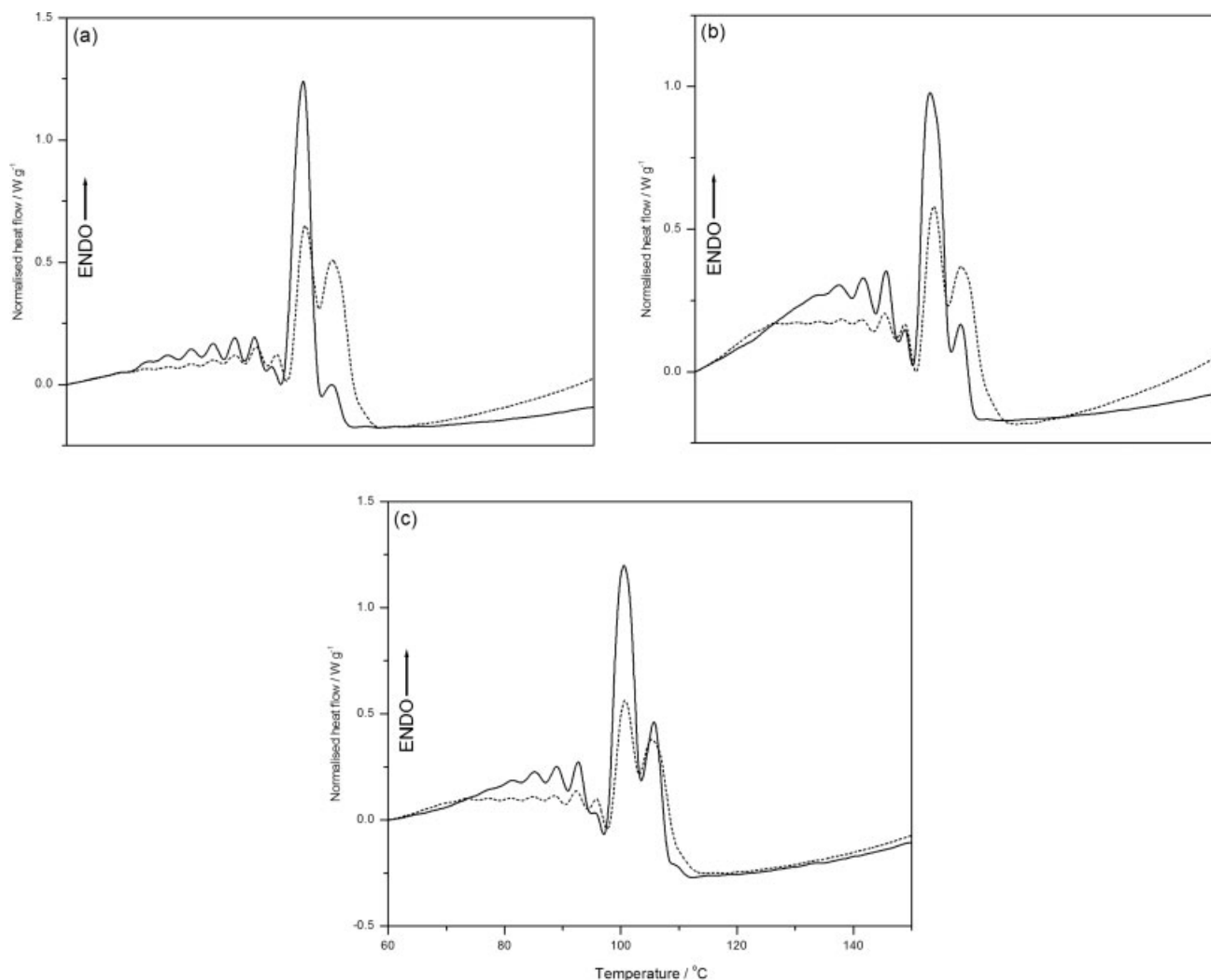


Figure 5 DSC heating curves, after thermal fractionation, of LDPE/H1 wax blends (solid line—experimental curves, broken line—calculated curves): (a) 90/10, (b) 80/20, and (c) 70/30 w/w.

in the crystalline phase. The melting enthalpies of LLDPE/H1 wax blends are higher than that of pure LLDPE (Table I), and no trend was observed with an increase in wax content. Because of the partial miscibility of LLDPE and H1 wax, the enthalpy was calculated for the combined wax and LLDPE peaks. This explains the higher enthalpy (crystallinity), because the more crystalline wax probably crystallizes in the amorphous parts of LLDPE. A decrease in enthalpy values with increasing wax content is observed when A1 wax is blended with LLDPE (Table I). This is probably the result of the lower crystallinity of A1 wax when compared with that of pure LLDPE.

The DSC melting curves for pure polyethylenes and waxes, obtained after thermal fractionation (stepwise cooling), are shown in Figure 2. All the curves show a series of melting peaks that depict the melting of crystallites of specific branching density.¹¹ It can be seen that pure A1 wax shows more peaks than H1 wax. A probable explanation of this behavior is the oxygen-

containing groups found on the backbone chain of A1 wax, which may influence the fractional crystallization process in a similar way than the presence of branches would.¹⁴ Since HDPE and H1 wax contains mostly nonbranched content, and since Cser et al.¹⁶ reported that all polymers with nonbranched content, like HDPE or PP, do not show any thermal fraction effect, it explains the observation that there is not much difference between the normal DSC curve and the DSC curve obtained after stepwise cooling of HDPE and H1 wax. LDPE shows seven peaks in the temperature range 81–103°C, while hexene LLDPE shows 11 peaks in the temperature range 80–132°C. The highest melting peak temperatures of LDPE and LLDPE are 101 and 131°C, respectively. This indicates that LDPE, after thermal fractionation, displays a narrower crystallization temperature range than LLDPE, suggesting a narrower size distribution of crystallites for LDPE.

The DSC curves of the HDPE/wax blends, after thermal fractionation, are shown in Figures 3 and 4.

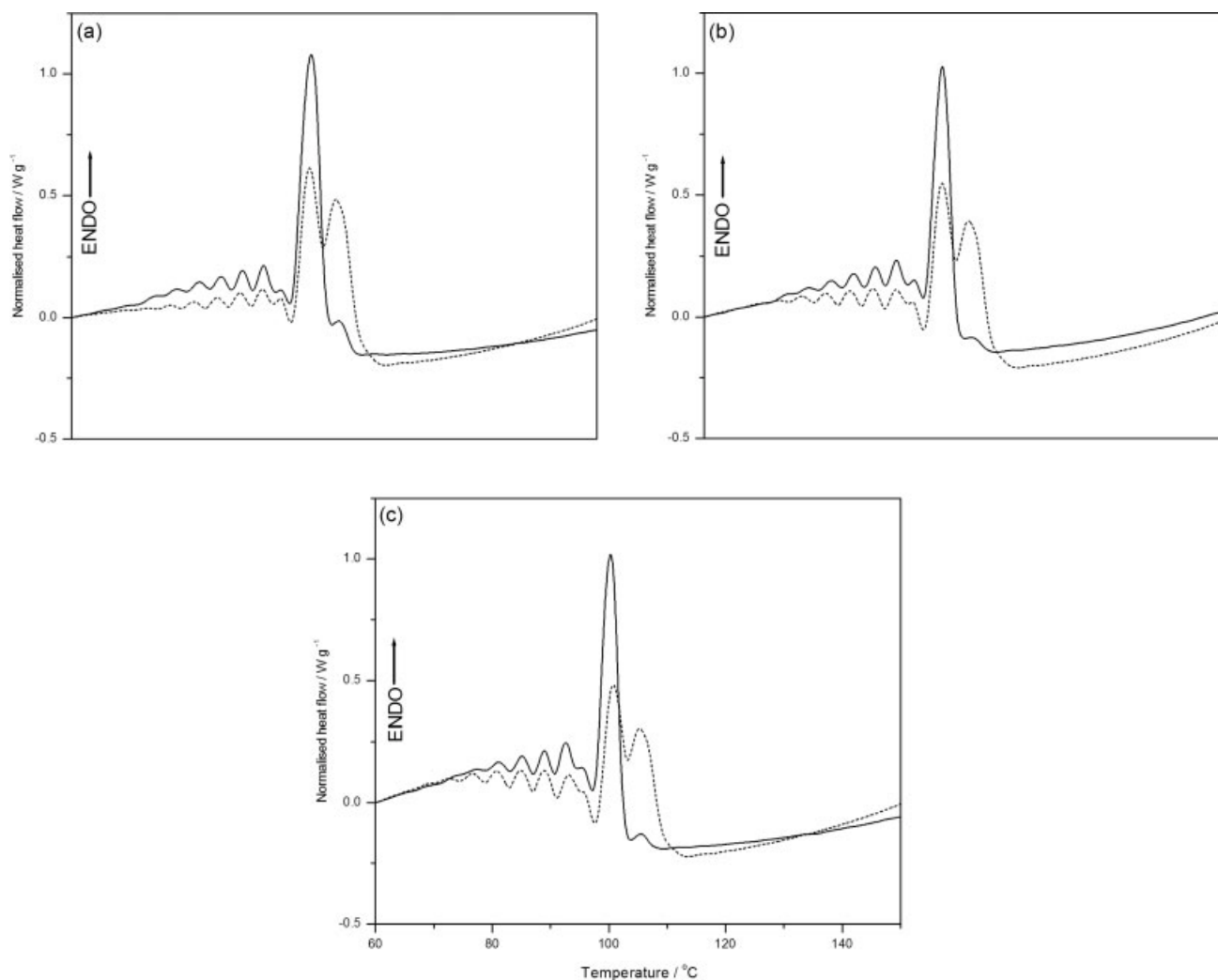


Figure 6 DSC heating curves, after thermal fractionation, of LDPE/A1 wax blends (solid line—experimental curves, broken line—calculated curves): (a) 90/10, (b) 80/20, and (c) 70/30 w/w.

The influence of blending was examined by comparison of the observed curves (solid line) with the calculated curves (dashed line). The calculated curves were obtained by adding the DSC curves, obtained after fractionation, of the individual components in the same proportion in which they were present in the blend. For the 90/10 and 80/20 w/w HDPE/H1 wax blends, it can be seen that the experimental melting curves for the blends are different from that of the calculated curves in the temperature range 60–100°C (Fig. 3). Figure 3(a) shows no peak in the experimental curve in this temperature region, while Figure 3(b,c) shows an increasingly pronounced peak. This confirms the increased phase separation with increasing wax content. The multiple peaks between 110 and 130°C support the possibility of cocrystal formation, while the dilution effect of wax on HDPE crystallization is clearly seen in the reduction of the melting temperature of the main HDPE fraction. HDPE/A1 wax blends (Fig. 4) show similar behavior as HDPE/H1

wax blends, except that in this case there is only a very slight indication of phase separation in the case of the 70/30 w/w blend, where the experimental melting curve show a broad flat peak between 60 and 100°C. These observations indicate better cocrystallization of A1 wax with HDPE. A1 wax does, however, have the same influence than H1 wax on the crystallization of the main polymer fraction.

Figures 5 and 6 show the DSC melting curves, after thermal fractionation, of the LDPE/wax blends. It is not possible from these curves to determine miscibility or cocrystallization of LDPE and wax chains, because the wax fraction peaks are in the same temperature region than the lower-temperature LDPE fraction peaks. The lower-temperature peaks in the experimental curves are, however, more intense than those in the theoretically predicted curves. This possibly indicates wax cocrystallization with the lower-temperature LDPE fractions. A clear dilution effect can be seen when comparing the high-temperature

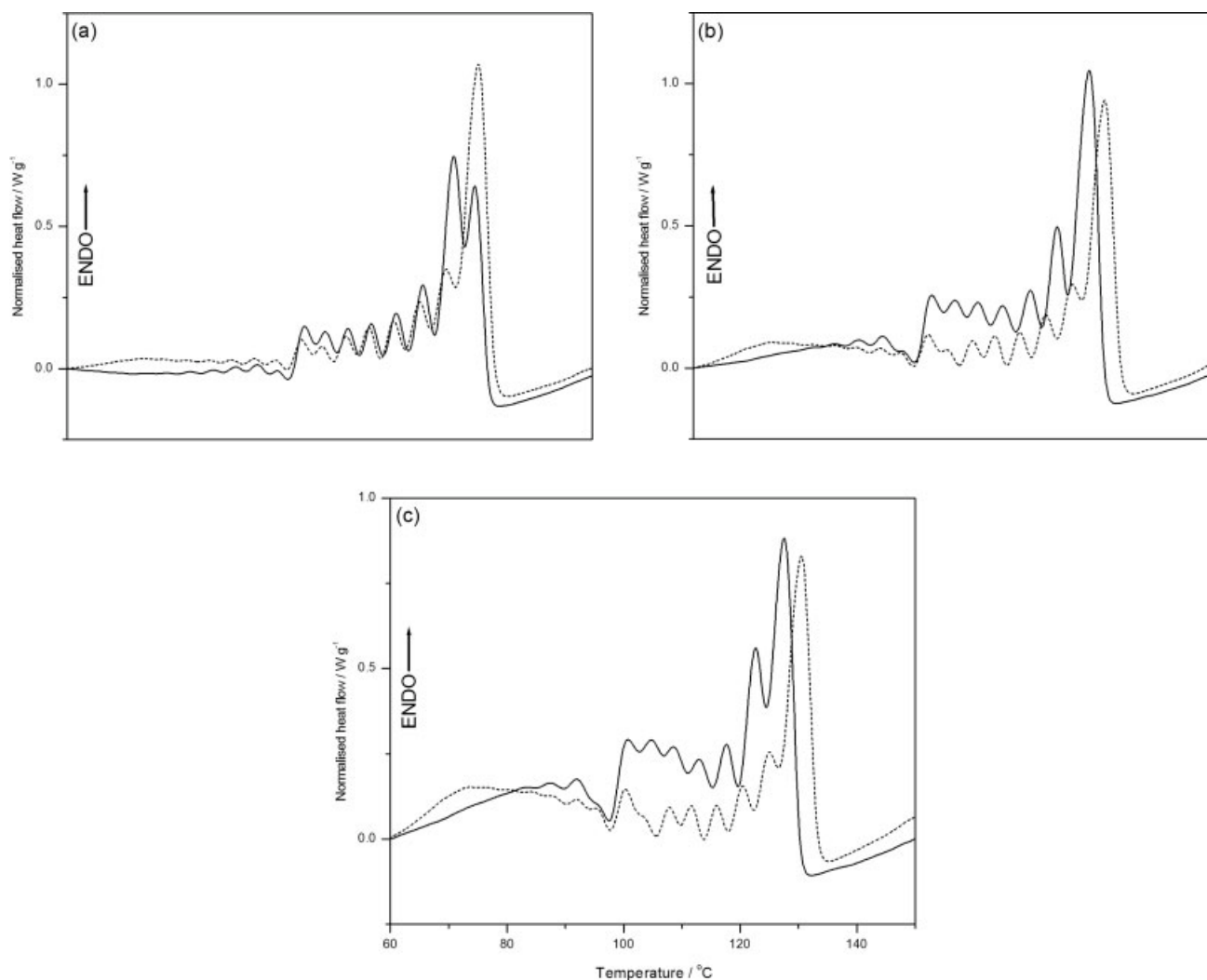


Figure 7 DSC heating curves, after thermal fractionation, of LLDPE/H1 wax blends (solid line—experimental curves, broken line—calculated curves): (a) 90/10, (b) 80/20, and (c) 70/30 w/w.

peaks in the experimental and theoretically predicted curves. A1 wax seems to strongly influence the crystallization of the highest temperature LDPE fraction, as is evident from the almost complete disappearance of this peak in the experimental curves in Figure 6.

Figures 7 and 8 show the DSC melting curves, after thermal fractionation, of the LLDPE/wax blends. All the curves contain a well-resolved series of melting peaks between 95 and 132°C, suggesting that independently melting crystallites are formed during stepwise cooling.¹⁴ H1 wax seems to be only partially miscible with LLDPE (Fig. 7), although there is a difference between the observed and theoretically predicted melting peaks of the wax fraction. It seems as if the shorter wax chains may have cocrystallized with LLDPE, while the longer chains crystallized separately in the LLDPE amorphous phase. The presence of H1 wax substantially influences the crystallization behavior of LLDPE. It not only dilutes the LLDPE crystals but also gives rise to a different crystal frac-

tion distribution, favoring lower temperature melting crystal fractions. A1 wax seems to influence the crystallization behavior of LLDPE in the same way as H1 wax, but A1 wax is clearly much more miscible with LLDPE than H1 wax, which is clear from the almost complete absence of fraction melting peaks in the experimental curves in the temperature region 60–90°C. This is probably the result of stronger interaction between LLDPE and A1 wax. In previous research by our group,¹⁰ it was shown that LLDPE and H1 wax cocrystallizes from solution for samples containing up to 50 wt % wax.

Table II summarizes the surface free energy data for all the blends. In the case of HDPE/H1 wax, the total surface free energy initially decreases and then increases, while the polar part slightly increases and then decreases with increasing wax content. This observation is in line with the miscibility trends observed with DSC. Krump et al.¹² showed that, in the absence of any other effects, miscibility between wax

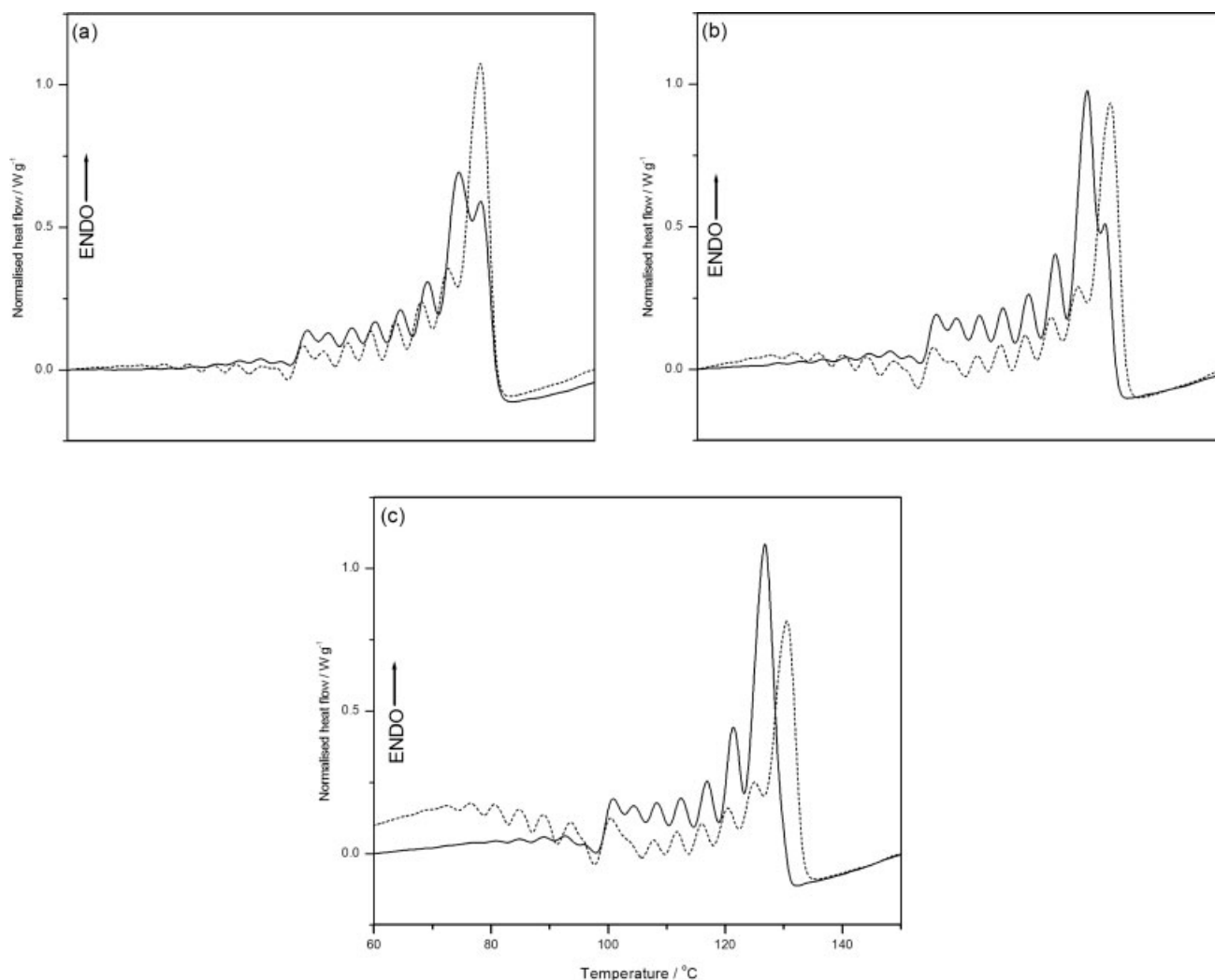


Figure 8 DSC heating curves, after thermal fractionation, of LLDPE/A1 wax blends (solid line—experimental curves, broken line—calculated curves): (a) 90/10, (b) 80/20, and (c) 70/30 w/w.

and PE causes a decrease in total surface free energy and an increase in its polar component. The opposite was observed with decreasing PE/wax miscibility. In the case of LDPE/H1 wax, the total surface free energy initially decreases and then increases, while the polar part slightly increases and then decreases with increasing wax content. This observation is in line with the miscibility trends observed with DSC. The surface free energy of the HDPE/A1 wax and LDPE/A1 wax blends, respectively, shows similar trends than the HDPE/H1 wax and LDPE/H1 wax blends that can be explained in a similar way. In these cases, however, the surface free energy values are higher, which is the result of the more polar character of A1 wax. LLDPE/A1 wax blends are miscible for all the investigated samples. This is clear from the continuously decreasing total surface free energy and increasing polar part with increasing wax content.¹² The polar part also increases as a result of the polar nature of A1 wax. In the case of the LLDPE/H1 wax

blends, there is, however, a continuous increase in total surface free energy and a continuous decrease in the polar part. This is in line with the partial miscibility of these blends observed in the DSC results.

The mechanical properties of the different blends are summarized in Table III. Young's modulus of the HDPE/wax blends slightly increased with an increase in wax content for both H1 wax and A1 wax. This is associated with the higher degree of crystallinity of the material when H1 wax is present, and the better miscibility (probably cocrystallization) in the case of A1 wax. The H1 wax blends generally show higher modulus values than the A1 wax blends, indicating that the modulus of H1 wax is higher than that of A1 wax. This is associated with the higher degree of crystallinity of H1 wax when compared with that of A1 wax. Despite the increasing crystallinity of the HDPE/wax blend, a slight decrease in yield stress with an increase in wax content is observed. Wax type and content do not seem to have any influence

TABLE II
Total Surface Free Energy, as Well as Its Disperse and Polar Parts, of the Pure Polyethylenes and Waxes, and their Blends

Sample	Surface free energy/mJ m ⁻²		
	γ_{total}	γ_{LW}	γ_{AB}
HDPE	30.4 ± 2.3	29.9 ± 2.3	1.0 ± 0.2
LDPE	31.1 ± 2.1	30.4 ± 1.7	0.7 ± 0.3
LLDPE	31.2 ± 0.7	29.4 ± 0.5	0.6 ± 0.2
H1 wax	29.4 ± 3.1	29.0 ± 3.1	0.4 ± 0.4
A1 wax	37.6 ± 5.2	29.6 ± 5.0	8.0 ± 1.3
HDPE/H1 wax (90/10 w/w)	34.0 ± 3.9	31.7 ± 3.7	3.3 ± 1.1
HDPE/H1 wax (80/20 w/w)	32.2 ± 4.0	28.5 ± 3.7	3.8 ± 1.5
HDPE/H1 wax (70/30 w/w)	35.6 ± 3.5	34.4 ± 3.4	1.2 ± 0.7
HDPE/A1 wax (90/10 w/w)	29.8 ± 4.7	27.6 ± 4.5	2.2 ± 1.4
HDPE/A1 wax (80/20 w/w)	28.9 ± 3.2	25.1 ± 2.8	3.8 ± 1.3
HDPE/A1 wax (70/30 w/w)	30.3 ± 3.1	29.4 ± 1.3	0.9 ± 0.2
LDPE/H1 wax (90/10 w/w)	26.6 ± 3.4	23.2 ± 3.1	3.4 ± 1.3
LDPE/H1 wax (80/20 w/w)	27.6 ± 4.3	25.4 ± 4.1	2.2 ± 1.3
LDPE/H1 wax (70/30 w/w)	29.4 ± 2.5	27.5 ± 2.0	1.9 ± 1.0
LDPE/A1 wax (90/10 w/w)	38.1 ± 2.1	32.7 ± 2.0	5.4 ± 0.9
LDPE/A1 wax (80/20 w/w)	36.6 ± 2.5	32.4 ± 2.4	4.2 ± 0.9
LDPE/A1 wax (70/30 w/w)	40.5 ± 4.3	38.2 ± 2.4	2.3 ± 1.1
LLDPE/H1 wax (90/10 w/w)	30.0 ± 4.2	27.7 ± 4.0	2.3 ± 1.3
LLDPE/H1 wax (80/20 w/w)	32.4 ± 2.9	30.9 ± 2.8	1.5 ± 0.7
LLDPE/H1 wax (70/30 w/w)	32.6 ± 4.5	31.5 ± 4.0	1.1 ± 0.9
LLDPE/A1 wax (90/10 w/w)	35.1 ± 1.8	32.7 ± 1.6	2.4 ± 0.8
LLDPE/A1 wax (80/20 w/w)	34.3 ± 5.0	31.2 ± 4.5	3.1 ± 2.0
LLDPE/A1 wax (70/30 w/w)	33.4 ± 3.7	29.7 ± 3.6	3.7 ± 1.0

γ_{total} , total surface free energy; γ_{LW} , disperse part; γ_{AB} , polar part.

on the elongation at yield of these blends. Both H1 wax and A1 wax reduce stress at break of the blends. The tensile strength at break generally depends on the polymer or material structure in a complicated way. Shorter chains in the materials imply that low elongation is needed to stretch the molecules and the chains are easier to draw from the lamellae. For the material to break, the tie chains should be tightly stretched, and the tightly stretched tie chains should be drawn out of the lamellae. It is well-known that the strength of semicrystalline polymers depends on the number of tie chains. Because of shorter wax chains probably cocrystallizing with HDPE, the average tie chain concentration decreases with increasing amount of wax. In this case, A1 wax seems to reduce the stress at break more than H1 wax. The only possible explanation for this behavior is the substantially lower crystallinity of A1 wax, which reduces the total crystallinity and the ultimate strength of the blend. Young's modulus increased with an increase in wax content for LDPE and LLDPE blended with both H1 wax and A1 wax. For a particular wax content, the values decrease in the order LLDPE/H1 wax > LLDPE/A1 wax > LDPE/H1 wax > LDPE/A1 wax. This is the result of LLDPE having a higher crystallinity than LDPE, and H1 wax having a higher crystallinity than A1 wax. A slight increase in yield stress for all the LDPE/wax and LLDPE/wax blends with increasing wax content is observed. An explanation

for this behavior is associated with an increase in the degree of crystallinity of these particular blends, since yield stress is a function of crystallinity. It can be seen that the increase is more pronounced in the case of H1 wax. Very little influence of wax type and content on the elongation at yield of LLDPE is observed. There is, however, a pronounced influence in the case of LDPE, where the strain at yield decreases with increasing wax content. Since movement of chains mainly occurs in the amorphous part of the polymer, LDPE is expected to have a much higher elongation at yield than LLDPE. Wax crystals in the amorphous phase will, however, restrict chain mobility. Both the DSC and thermal fractionation results strongly indicate wax crystallization in the amorphous phase of LDPE, which explains the pronounced decrease in elongation at yield with increasing wax content. The decrease is more pronounced in the case of H1 wax. The reason for this is not clear, because one would expect stronger interaction between the oxygen-containing groups in A1 wax and the LDPE chains, which would further reduce the LDPE chain mobility. This observation can, however, be explained through the lower crystallinity of A1 wax, giving rise to fewer wax crystals in the LDPE amorphous phase. Both H1 wax and A1 wax reduce stress at break of the blends. It is further obvious that the difference between the yield stress and stress at break of LLDPE decreased quite substantially with increasing wax content, indi-

TABLE III
The Mechanical Properties of Polyethylenes, Waxes, and Their Blends

Sample PE/wax	$\varepsilon_y \pm S\varepsilon_y$ (%)	$\sigma_y \pm S\sigma_y$ (MPa)	$\varepsilon_b \pm S\varepsilon_b$ (%)	$\sigma_b \pm S\sigma_b$ (MPa)	$E \pm sE$ / MPa
HDPE	17.5 ± 0.3	27.1 ± 0.4	886.0 ± 16.4	25.4 ± 2.6	332.7 ± 12.3
LDPE	49.7 ± 1.3	9.1 ± 0.1	539.5 ± 6.5	9.4 ± 0.4	94.8 ± 2.1
LLDPE	22.2 ± 0.9	12.3 ± 0.1	1216.0 ± 55.2	27.1 ± 0.7	111.8 ± 4.7
HDPE/H1 wax (90/10 w/w)	17.3 ± 0.3	27.2 ± 0.5	712.0 ± 33.6	13.1 ± 1.4	334.1 ± 15.5
HDPE/H1 wax (80/20 w/w)	17.5 ± 0.4	26.6 ± 0.4	158.2 ± 18.1	12.9 ± 2.3	340.1 ± 14.6
HDPE/H1 wax (70/30 w/w)	20.4 ± 0.7	24.7 ± 0.3	28.9 ± 1.5	10.3 ± 1.4	354.0 ± 3.5
HDPE/A1 wax (90/10 w/w)	19.3 ± 0.3	23.8 ± 0.7	566.7 ± 55.6	10.1 ± 1.7	354.0 ± 15.5
HDPE/A1 wax (80/20 w/w)	17.7 ± 0.8	23.0 ± 0.5	29.8 ± 3.6	7.9 ± 1.2	334.1 ± 14.6
HDPE/A1 wax (70/30 w/w)	19.1 ± 0.1	21.4 ± 0.3	7.4 ± 0.9	5.3 ± 1.1	340.4 ± 3.5
LDPE/H1 wax (90/10 w/w)	25.0 ± 0.7	10.4 ± 0.2	81.2 ± 1.7	2.5 ± 0.2	134.2 ± 3.2
LDPE/H1 wax (80/20 w/w)	21.3 ± 0.3	12.2 ± 0.5	54.2 ± 3.1	4.7 ± 0.8	141.7 ± 7.2
LDPE/H1 wax (70/30 w/w)	18.6 ± 0.2	12.9 ± 0.2	31.7 ± 2.2	1.2 ± 0.3	154.3 ± 2.5
LDPE/A1 wax (90/10 w/w)	28.7 ± 0.5	8.7 ± 0.1	88.9 ± 9.4	1.9 ± 0.6	100.2 ± 1.9
LDPE/A1 wax (80/20 w/w)	25.6 ± 0.2	8.9 ± 0.1	72.9 ± 5.0	2.2 ± 0.6	107.8 ± 1.0
LDPE/A1 wax (70/30 w/w)	22.8 ± 0.5	9.5 ± 0.1	43.8 ± 1.3	1.5 ± 0.6	129.2 ± 2.3
LLDPE/H1 wax (90/10 w/w)	21.4 ± 0.9	14.8 ± 0.4	990 ± 11.9	22.2 ± 0.6	187.8 ± 5.4
LLDPE/H1 wax (80/20 w/w)	20.7 ± 1.5	15.4 ± 0.3	999.2 ± 36.1	19.9 ± 2.0	192.4 ± 13.9
LLDPE/H1 wax (70/30 w/w)	17.3 ± 0.4	16.1 ± 0.5	960.6 ± 49.0	17.3 ± 1.2	201.7 ± 15.3
LLDPE/A1 wax (90/10 w/w)	21.9 ± 0.5	13.0 ± 0.1	1024.4 ± 40.7	22.5 ± 0.4	148.2 ± 8.7
LLDPE/A1 wax (80/20 w/w)	21.8 ± 0.3	13.1 ± 0.1	1006.0 ± 21.4	20.8 ± 0.3	158.0 ± 10.3
LLDPE/A1 wax (70/30 w/w)	19.9 ± 0.3	14.6 ± 0.1	1004.2 ± 13.9	18.5 ± 0.3	161.8 ± 10.7

ε_y , σ_y , ε_b , σ_b , and E are elongation at yield, yield stress, elongation at break, stress at break, and Young's modulus of elasticity; $S\varepsilon_y$, $S\sigma_y$, $S\varepsilon_b$, $S\sigma_b$, and S_E are their standard deviations.

cating that the presence of wax may reduce strain hardening.

CONCLUSIONS

Melt-mixing of HDPE with wax gave rise to a completely miscible blend for both 10 and 20% wax contents. This miscibility is probably the result of cocrystallization of the wax with HDPE, which is clear from the absence of low-temperature peaks in the normal DSC curves, and in the DSC curves obtained after thermal fractionation. A wax content of 30% gave rise to a partially miscible blend. This is clear from the development of a lower temperature melting peak in the DSC curve, and from the thermal fractionation curves that show a similarity between the calculated and experimental curves in the temperature range 60–100°C. These observations were further supported by the surface free energy results. The presence of wax had very little influence on the modulus and yield point of HDPE, probably because the two components have similar crystallinity (in the case of H1 wax) and cocrystallize to a large extent. However, the presence of wax caused a substantial decrease in both stress and strain at break of the blends. The reason for this is that cocrystallization of HDPE and wax, combined with the fact that the wax has very short chains when compared with HDPE, caused a reduction in the tie chain concentration of the crystallites.

Complete miscibility was observed for all the LLDPE/A1 wax blends. This indicates probable cocrystallization of A1 wax with LLDPE, which is also

evident from the thermal fractionation curves. LLDPE/H1 wax blends were, however, partially miscible for all wax contents. These conclusions were also supported by the surface free energy results. Melt-mixing of LDPE with H1 wax gave rise to a partially miscible blend for all wax contents investigated, while complete miscibility was observed for the 90/10 w/w LDPE/A1 wax blend, but not for the blends containing higher A1 wax contents. The reason for this observation is probably because the wax crystallized mostly in the amorphous part of LDPE, although there may have been some cocrystallization. The partial miscibility was also clear from the surface free energy results. As in the case of HDPE/wax blends, changes in the tensile properties could be explained in terms of the miscibility and proposed morphologies of the LLDPE/wax and LDPE/wax blends.

References

1. Krupa, I.; Luyt, A. S. *Polym Degrad Stab* 2000, 70, 111.
2. Krupa, I.; Luyt, A. S. *J Appl Polym Sci* 2001, 81, 973.
3. Krupa, I.; Luyt, A. S. *Polym Degrad Stab* 2001, 73, 157.
4. Krupa, I.; Luyt, A. S. *Polymer* 2001, 42, 7285.
5. Mtshali, T. N.; Luyt, A. S.; Krupa, I. *Thermochim Acta* 2001, 380, 47.
6. Krupa, I.; Luyt, A. S. *S Afr J Chem* 2002, 55, 52.
7. Djokovic, V.; Mtshali, T. N.; Luyt, A. S. *Polym Int* 2003, 52, 999.
8. Hlangothi, S. P.; Krupa, I.; Djokovic, V.; Luyt, A. S. *Polym Degrad Stab* 2003, 79, 53.
9. Mtshali, T. N.; Van Sitter, C. G. C. E.; Djokovic, V.; Luyt, A. S. *J Appl Polym Sci* 2003, 89, 2446.
10. Luyt, A. S.; Brúll, R. *Polym Bull* 2004, 52, 177.

11. Novak, I.; Krupa, I.; Luyt, A. S. *J Appl Polym Sci* 2005, 95, 1164.
12. Krump, H.; Luyt, A. S.; Molefi, J. A. *Mater Lett* 2005, 59, 517.
13. Galante, M. J.; Mandelkern, L.; Alamo, R. G. *Polymer* 1998, 39, 5105.
14. Shanks, R. A.; Amarasinghe, G. *Polymer* 2000, 41, 4579.
15. Drummond, K. M.; Hopewell, J. L.; Shanks, R. A. *J Appl Polym Sci* 2000, 78, 1009.
16. Cser, F.; Hopewell, J. L.; Tajne, K.; Shanks, R. A. *J Therm Anal Calorim* 2000, 61, 687.
17. Liu, W.; Kim, S.; Lopez, J.; Hsiao, B.; Keating, M.Y.; Lee, I.-H.; Landes, B.; Stein, R.S. *J Therm Anal Calorim* 2000, 59, 245.
18. Shanks, R. A.; Amarasinghe, G.; *J Therm Anal Calorim* 2000, 59, 471.
19. Chen, F.; Shanks, R. A.; Amarasinghe, G. *Polymer* 2001, 42, 4579.
20. Arnal, M. L.; Canizales, E.; Müller, A. J. *Polym Eng Sci* 2002, 42, 2048.
21. Müller, A. J.; Arnal, M. L.; Spinelli, A. L.; Canizales, E.; Puig, C.C.; Wong, H.; Han, C.C. *Macromol Chem Phys* 2003, 204, 1297.
22. Amarasinghe, G.; Shanks, R. A. *J Therm Anal Calorim* 2004, 78, 349.
23. Müller, A. J.; Arnal, M. L. *Prog Polym Sci* 2005, 30, 559.
24. Hato, M. J.; Luyt, A. S. *J Appl Polym Sci* 2005, 96, 1748.